

ERDA with swift heavy ions for materials characterization

D. K. Avasthi^{*,†} and W. Assmann^{**}

^{*}Nuclear Science Centre, Post Box 10502, Aruna Asaf Ali Marg, New Delhi 110 067, India

^{**}Sektion Physik, Universität München, 85748 Garching, Germany

Elastic recoil detection analysis (ERDA) is a technique specially suited for depth profiling of light elements, which overcomes the limitations of Rutherford backscattering (RBS). The developments in the technique enabled depth profiling of elements from hydrogen up to very heavy elements with single element resolution in the light mass region. The use of large area position sensitive telescope detectors made it a highly sensitive technique with which ion beam induced modifications such as interface mixing, electronic sputtering and radiation damage studies can be performed during irradiation itself.

1. Introduction

THE first nuclear particle accelerator was built in early 1930s with the aim to probe into the nucleus by nuclear reactions. With the passage of time, it was realized that accelerators can play an important role in other branches of science. Materials science gained a lot by accelerators. Ion implanters, which are basically low energy (typically 400 keV) accelerators are today essential tools in semiconductor technology. Alpha particles of energy of a few MeV have been playing a major role in materials characterization by Rutherford backscattering (RBS)¹ and channeling². RBS provides depth profiling of elements in the surface region up to a few microns. RBS channeling measurements allow³ the quantification of crystallization, dopant atom location, determination of strain in superlattices, etc. RBS, however, has poor sensitivity for the detection of light elements (C, N, O, etc.) especially in the presence of a substrate of higher mass (such as Si, which is often the case). This is because of low Rutherford scattering cross section which is proportional to the product of the atomic numbers of the projectile and the scatterer. Another limitation of RBS is its inability to detect hydrogen because no projectile can get scattered back from this lightest element. The disadvantages of RBS are overcome by another technique called elastic recoil detection analysis (ERDA)⁴ first demonstrated by L'Ecuyer *et al.* in 1976. The breakthrough of the ERDA technique came when heavy ion accelerators became

available for materials research. Basically ERDA is a technique quite similar to RBS, but instead of scattered projectile detection at the back angle, the recoils are detected (resulting from elastic collision of the incident particle and the atoms in the sample) in forward direction. Its use for hydrogen depth profiling was demonstrated⁵ by Doyle and Peercey. ERDA technique further got strengthened in terms of its capabilities by the use of particle identifying techniques, which were commonly used by experimental nuclear physicists. Salient features of ERDA with high energy heavy ions are:

- (i) Large recoil cross sections with heavy ions and hence good sensitivity.
- (ii) Almost same recoil cross section for a wide mass range of target atoms.
- (iii) Element depth profiling of a wide range of elements from hydrogen to rare earth elements using particle identifying techniques.

2. Principles of ERDA

In an elastic collision of the incident particle of mass m_p (in atomic mass units) and energy E_p , with the atom of mass m_r (in atomic mass units) present in the sample, the atom in the sample which is at rest, recoils in forward direction after the collision. The energy of the recoiling atom can be derived from the basic principle of conservation of energy and momentum. The recoil energy E_r of atom with mass m_r at an angle ϕ with respect to the beam direction is given by

$$E_r = kE_p, \quad (1)$$

where k is kinematic factor given by

$$k = 4m_p m_r \cos^2 \phi / (m_p + m_r)^2. \quad (2)$$

The projectile mass, its energy and recoil angle remains fixed under a given experimental condition, therefore atoms of different masses in the sample come out with different recoil energies as governed by eq. (1). If $m_p > m_r$, projectiles can only be scattered in a limited angular range with a maximum angle θ defined by

[†]For correspondence. (e-mail: dka@nsc.ernet.in)

SURFACE CHARACTERIZATION USING ACCELERATORS

$\theta = \arcsin(m_r/m_p)$. This fact can be used to avoid scattered projectiles by placing the detector for the recoils beyond this angle. Normally the heavier scattered projectiles or recoils of the sample are stopped in a stopper foil of appropriate thickness in front of the detector. Light element recoils are not stopped in the stopper foil due to smaller energy loss during traversal. Figure 1 shows the schematic of an ERDA set up and explains the principle of ERDA.

2.1 Quantification

The concentration of sample atoms N_r (in atoms/cm²) can be determined by the following relation

$$N_r = Y \sin \alpha / (N_p \Omega d \sigma / d\Omega), \quad (3)$$

where Y is the number of recoils detected in the detector subtending a solid angle of Ω , N_p is the number of incident ions, α is the sample tilt angle as seen in Figure 1, $d\sigma/d\Omega$ is the Rutherford recoil cross section given by

$$d\sigma/d\Omega = [Z_p Z_r e^2 (m_p + m_r)]^2 / (4 E_p^2 m_r^2 \cos^3 \phi), \quad (4)$$

where Z_p and Z_r are the atomic numbers of the projectile ion and the recoiling ion from the sample respectively.

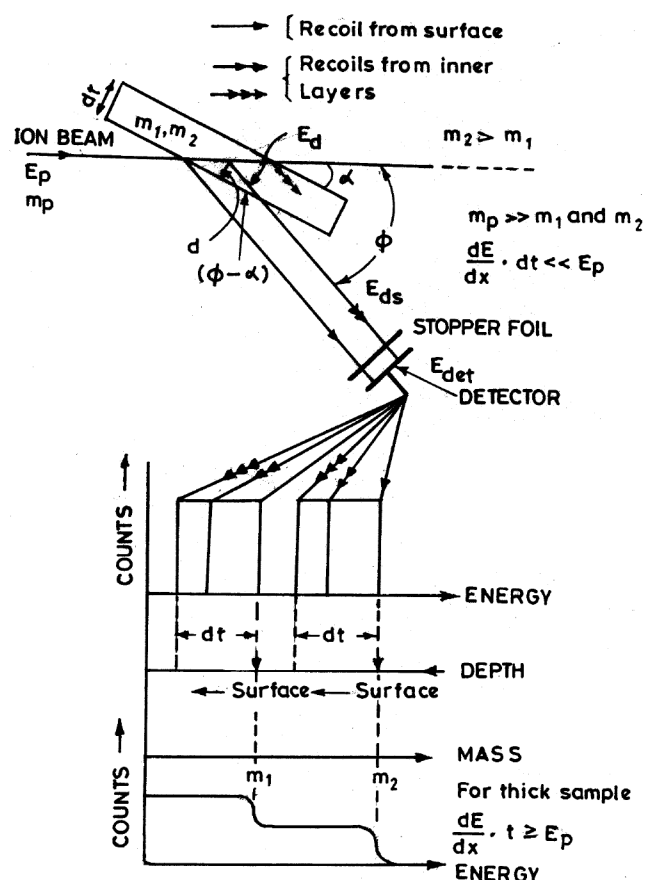


Figure 1. Schematic diagram indicating the principle of ERDA.

2.2 Depth profiling

The energy of recoils as detected by the detector depends on (i) the kinematics as per eq. (1), (ii) the energy loss of the incoming ion in the sample material up to a certain depth d , (iii) the energy loss of the recoil within the sample from depth d , where it originates, and (iv) the energy loss of the recoil atom in the stopper foil as depicted in Figure 1. If the recoil originates from the surface, the energy of the recoil atom is determined only by the kinematics according to eq. (1). This is the maximum energy of a recoil of particular mass originating from the sample's surface. The energy of a recoil ion generated at depth d is given by

$$E_d = k[E_p - (d/\sin \alpha)(dE/dx)_{in}], \quad (5)$$

where $(dE/dx)_{in}$ is the energy loss of incoming ion in the sample material.

The energy of recoil E_{ds} , originating at depth d , coming out at the surface is

$$E_{ds} = E_d - \{d/\sin(\phi - \alpha)\}(dE/dx)_{out}, \quad (6)$$

where $(dE/dx)_{out}$ is the energy loss of recoil in the sample. The recoil energy as detected by the detector is given by

$$E_{det} = E_{ds} - \Delta E_{foil}(E_{ds}), \quad (7)$$

where ΔE_{foil} is the energy loss of recoil in the foil, which is dependent on energy.

The recoil energy is converted to depth scale using the eqs (5) to (7) given above.

2.3 Mass identification

Recoil energy provides the information about the mass of the elements in the sample as per eq. (1) at fixed ϕ . The identification of the elements from the recoil energy is possible as long as the recoil energy difference of the elements is larger than the energy resolution of the set up. Higher mass recoils have higher energy as per eq. (1), if $m_p > m_r$ and appear as separate groups as shown in Figure 1.

2.4 Sensitivity

Sensitivity is defined as the minimum quantity of an element, which can be detected for a moderate charge of incident ions (say 10 μ C). It is dependent on the recoil cross section and the detector solid angle. The latter is kept normally in such a way that the opening of detector has an acceptance angle, which is comparable or

smaller than the kinematic broadening. Typically, the minimum detection limit is about 0.1 atomic per cent.

2.5 Depth resolution

Depth resolution depends on the energy resolution dE , which is governed by various factors such as (i) incident ion beam energy spread, (ii) straggling in the stopper foil and the detector system, (iii) inhomogeneities in the stopper foil and the entrance window of the detector, (iv) detection system resolution, which is composed of the electronics noise and the detector resolution, (v) kinematic broadening, and (vi) angular and lateral spread due to multiple scattering, which adds to the kinematic broadening. Incident beam resolution is typically 50 keV. Detection system resolution is typically 1% and is therefore about 200 keV for 20 MeV heavy ion recoils. One has to choose the experimental parameters in such a way that the recoil energy spread due to various factors is minimized.

3.0 ERDA in different geometries

3.1 ERDA in transmission geometry without stopper foil

ERDA can be employed in transmission geometry as shown at the top left inset in Figure 2. It is suited only for the self-supporting thin film samples. There have been a few such studies⁶⁻⁸, where the impurities in self-supporting thin foils used in nuclear physics experiments, were determined by ERDA technique.

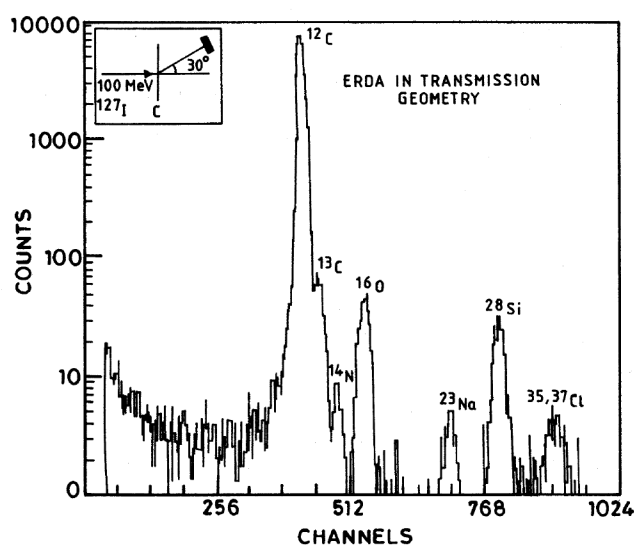


Figure 2. Recoil spectrum of a C foil irradiated with 100 MeV I ions. (Reprinted from *Nucl. Instrum. Methods*, Volume number A334, Jaipal *et al.*, Characterization of targets, p. 196, Copyright (1993), with permission from Elsevier Science.)

A self-supporting thin C foil ($100 \mu\text{g}/\text{cm}^2$) was bombarded by 100 MeV I ions and the recoils were detected in a surface barrier detector placed at 30 degrees. The maximum scattering angle for ^{127}I projectile on C atom is 5.4 degree. Therefore the scattered ions do not reach the detector kept at 30° . The recoils of N, O, Na and Cl apart from C were seen as shown in Figure 2 and their concentrations were determined⁶.

In another experiment, effectiveness of an in-vacuum transfer system was examined by studying a thin Ca target kept in vacuum during transfer and later exposed to air for a short duration. The recoils from Ca thin foil (transferred from evaporator to ERDA chamber under vacuum) were recorded in a surface barrier detector at an angle of 42° using 100 MeV Ag ions. The maximum scattering angle of Ag ions on Ca is 21.9 degree. The experiment was repeated when such a Ca film was exposed to air for a small duration (about a minute). The recoil spectra⁷ in the two cases are shown in Figure 3, which clearly indicates low contamination of oxygen in the case of in-vacuum target transfer system. It helped to check an indigenously designed load lock system.

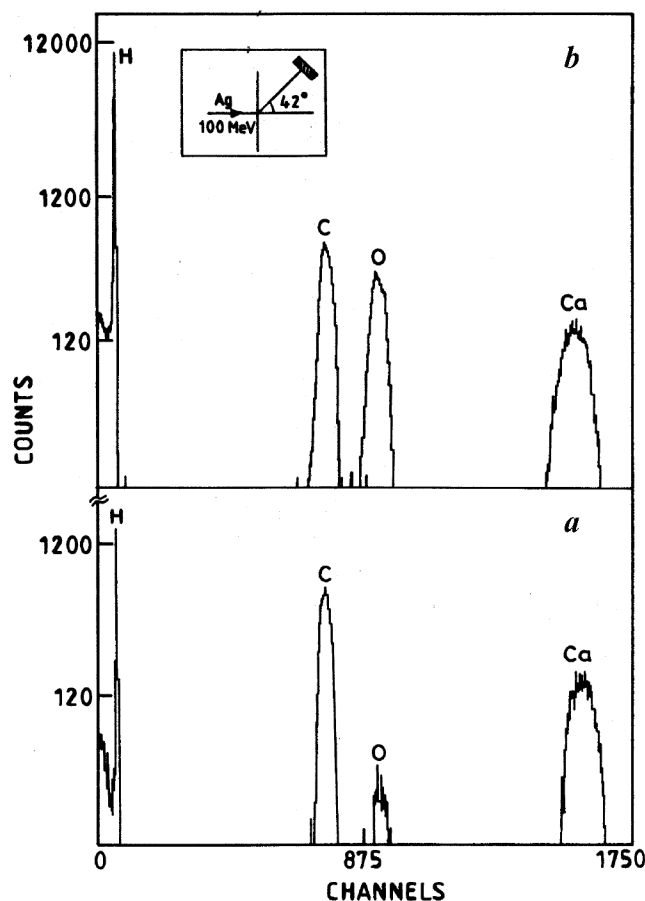


Figure 3. Recoil spectra of a Ca target for (a) in-vacuum transfer conditions and (b) after exposure to air. (Reprinted from *Nucl. Instrum. Methods*, Volume number A362, Kabiraj, D. *et al.*, In vacuum target transfer facility, p. 205, Copyright (1995), with permission from Elsevier Science.)

Most of the cases of materials science interest, however, have samples of thin films on thick substrate or thick samples, where the transmission geometry cannot be utilized. In such cases, one has to adopt the reflection geometry as discussed in the following section.

3.2 ERDA in reflection geometry

In this geometry the sample is tilted at an angle and the detector is kept at an angle greater than the sample tilt angle as already shown in Figure 1. This is the most common geometry for ERDA experiments. Various developments and examples involving this setup are discussed in the following sections.

3.2.1 Hydrogen depth profiling: Hydrogen has high diffusivity in materials. Its presence affects the properties of such materials. Therefore hydrogen detection and depth profiling is of wide interest. Among various cases of interest, we discuss here hydrogen depth profiling of Non Evaporable Getter (NEG) material, an alloy of V, Fe and Zr. It has the property of absorbing the gases after its activation and is of interest in vacuum technology. Since hydrogen is one of the main residual gases in vacuum, it was our interest to quantify the absorbed H in the NEG strip used in vacuum pumping⁹. Therefore we performed H depth profiling¹⁰ of a pristine NEG strip and the one used in vacuum pumping. 80 MeV Ni ions were incident on such a sample and the recoils were collected at an angle of 45°. The H recoil spectra are shown in Figure 4, which indicate considerable amount of H absorption in the NEG strip due to vacuum pumping action.

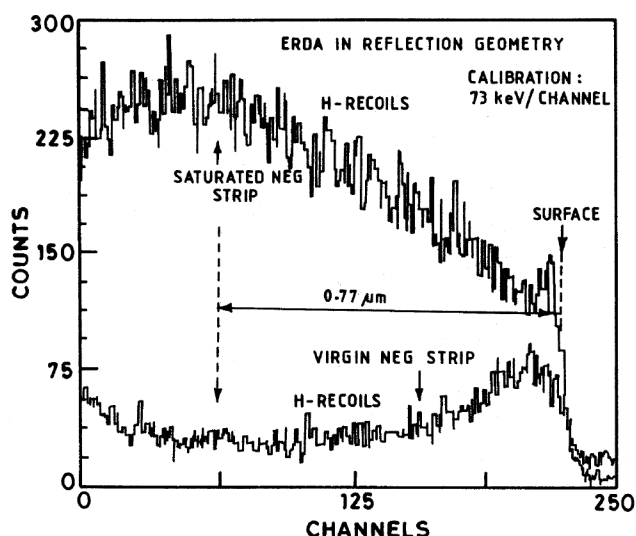


Figure 4. Recoil spectrum of H in pristine and saturated NEG strip. (Reprinted with permission from Trans Tech Publication Ltd. from *Materials Science Forum*, 1997, 248–29, 405.)

3.2.2 Multi-element analysis by ERDA. We will consider here an example¹¹ of stoichiometric analysis of a thin a-SiN_x:H film on Fe substrate. The film was made on Fe substrate instead of Si substrate as the interest was to detect the content of Si apart from H and N in the film. Such amorphous silicon nitride films have applications in gate insulators and in device passivation. The sample was tilted at an angle of 20° and detector was kept with a stopper foil of 6 μm in front of it to stop unwanted Fe recoils and scattered Ni ions, which were used as incident ion beam. The recoil spectrum obtained at 34° is shown in Figure 5, where the recoils of H, N and Si can be distinguished. From this spectrum the film stoichiometry was extracted as H = 3.8 at. %, N = 20.4 at. % and Si = 75.7 at. %.

3.2.3 ERDA with telescope detector. The above-mentioned methods are suitable when the elements to be detected (for determination of concentration) are well separated in mass. If there are elements in the sample which have neighboring masses, the recoil energies overlap and it becomes difficult to distinguish such elements in the sample. In such a situation, it is of advantage to use one of the other particle identification techniques to discriminate different elements. The techniques are time of flight (TOF)^{12–16} spectrometer, ΔE–E detector telescope^{17–23}, magnetic spectrograph^{24,25}, Bragg curve spectrometer (BCS)^{26,27}. TOF is best suited for low recoil energies but has the disadvantage of low detection efficiency for hydrogen and other lighter mass elements. TOF setups use micro channel

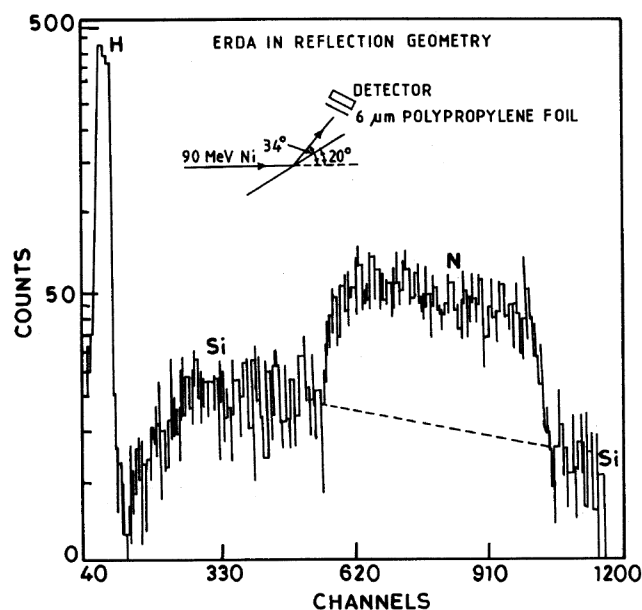


Figure 5. Recoil spectra of H, N and Si from a thin a-SiN_x:H film measured with 80 MeV Ni ions. (Reprinted from *Vacuum*, Avasthi, D. K., *et al.*, Hydrogen profiling and stoichiometry of an a-SiN_x:H film. p. 265, Copyright (1995), with permission from Elsevier Science.)

plates for timing signals, which are fragile and require careful handling and good vacuum conditions. BCS uses a relatively simple detector electronics but an additional detector is necessary if position sensitivity is desired. Also, detection of H is difficult with this technique. A magnetic spectrograph requires huge magnets and space for the same. It is expensive as well, but it provides the best possible resolution and is a good choice. Considering all this, the use of detector telescopes is an ideal choice for identifying neighbouring mass elements with good depth resolution. Such a set up can be designed and fabricated indigenously as per the requirement.

Telescope detectors²⁸ consist of two detectors. First one is used in transmission so that the recoils going through lose a fraction ΔE of their energy. Rest of the energy $E_{\text{rest}} = E - \Delta E$ is deposited in the second detector, which has such a thickness that the recoils get stopped in it. The recoil energies have to be high enough to overcome the detector entrance window and the transmission type ΔE detector. A schematic of such a set up is shown in Figure 6. The energy lost, ΔE in the first detector, depends on the atomic number and the mass of the recoil. Thus the energy lost by the recoils of different elements having almost identical energies is different and can be used to identify the atomic number of recoil. The signals are processed as shown in Figure 6. Total energy is obtained by adding the energies ΔE and $E - \Delta E$ obtained from the first and second detector after proper calibration of the electronic gains in the two detectors.

There are different possible configurations for telescope detectors. Using a transmission type thin solid state detector as ΔE detector and thick solid state detector as E_{rest} detector is one of the choices. Both these detectors are commercially available. The use of a gaseous detector (which can be fabricated as per the requirement) for ΔE is another choice coupled to a solid state detector as the E_{rest} detector. The third choice is using the gaseous detector for both the ΔE and E_{rest} measurements. The main advantage of the gaseous type detectors is that these are insensitive to radiation damage, rugged and can be fabricated indigenously. On the other hand, the solid state detectors are prone to radiation damage, besides being fragile (especially ΔE detectors) and are expensive. A typical gaseous detector telescope is shown in Figure 7.

The presence of N and O was determined²² in diamond like carbon (DLC) films using a telescope detector (having ΔE as gaseous type and E as solid state detector). It can be seen, for example that if 90 MeV Ni ions are incident on a DLC film having N and O as impurities, the recoil energies from the surface of the sample for C, N and O ions will be 32.6, 35.9 and 38.9 MeV respectively. Recoil energies of the atoms from various depth of the sample will overlap and cannot be distinguished by conventional ERDA. The ΔE part of the telescope detector, however, produces signals by which C, N and O recoils can be easily discriminated within the resolution capability of the detector. A two-dimensional ΔE - E spectrum of the recoils from the DLC sample is shown in Figure 8, giving a clear idea of potentiality of a detector telescope.

3.2.4 ERDA with large area position sensitive telescope detector. For many samples it is of importance to record the recoil spectrum with sufficient statistics us-

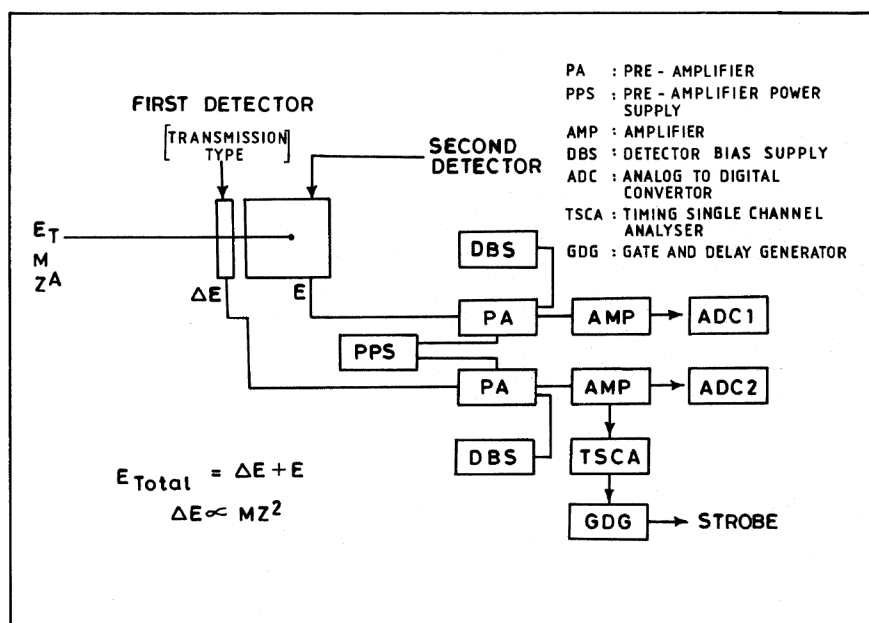


Figure 6. Set up of a ΔE - E telescope detector with electronics.

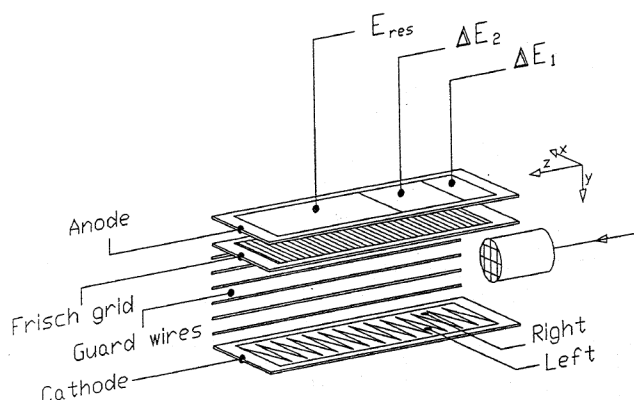


Figure 7. Schematic sketch of a gaseous telescope detector. E_{res} acts as the detector where all recoils are stopped and therefore its length is more as compared to ΔE detector. The pressure inside the detector volume is adjusted in such a way that the recoils of interest are stopped in the E_{res} section. Use of two ΔE part detectors allow analysis of very heavy masses.

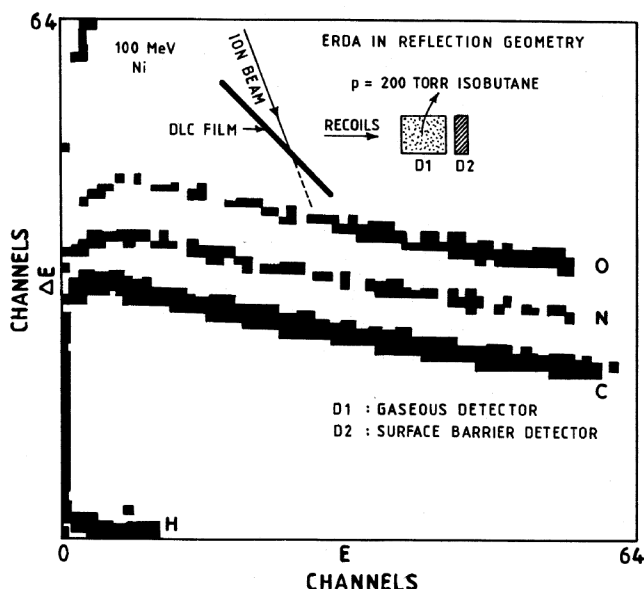


Figure 8. A two dimensional ΔE - E spectrum of recoils ejected from a DLC film with 90 MeV Ni ions. (Reprinted from *Nucl. Instrum. Methods*, Volume number B93, Avasthi, D. K. *et al.*, Simultaneous detection of light elements by ERDA with gas-ionization/Si ΔE - E detector telescope, p. 480, Copyright (1994), with permission from Elsevier Science.)

ing only a small dose of incident ions. This reduces the chance of radiation damage if, any, during the experiment for the analysis of the sample. To accomplish this objective, it is necessary to increase the solid angle by using a large area detector. The increase in the size of the detector increases the acceptance angle as well and results in larger kinematic broadening, which in turn deteriorates the depth resolution. The solution for this problem is a kinematic correction by measuring the actual scattering angle of the recoil. Assmann *et al.*²⁹ demonstrated the use of such a large area position sensi-

tive detector with the position sensitive feature in ERDA. The advantage of such a scheme was to increase the sensitivity without compromising the depth resolution. It became so popular that other accelerator laboratories having high energy heavy ions developed similar detectors^{30,31}. Such a detector system has recently been installed and tested in the materials science beam line (Figure 9) of NSC. The kinematic correction option by software will be implemented in the near future.

4.0 ERDA channeling and blocking measurements

4.1 ERDA blocking experiments

Blocking is a phenomenon, in which the recoils get blocked in crystallographic directions and therefore if one records these recoils in the axial direction by a two-dimensional position sensitive detector, a 'shadow' of the crystal axis appears, which is referred to as blocking pattern. A sample with high crystallinity is expected to give a blocking pattern with a sharp contrast of the axes and the region other than that. The blocking pattern of an amorphous sample will not show any axes. The contrast of the axis with the background gives an idea of the crystallinity of the sample under investigation. ERD blocking has been used by Huber *et al.*^{32,33} to investigate the radiation damage induced by swift heavy ions in semiconductor crystals. The advantage of this technique is the simultaneous use of the projectiles to cause damage as well as probe the sample. Figure 10 shows the blocking picture of an Si sample after irradiation with 210 MeV ¹²⁷I ions. The existence of the axes in the blocking pattern indicates that Si crystal retains the crystallinity even after irradiation.

4.2 ERDA channeling experiments

Channeling experiments in ERDA geometry with energetic heavy ion beams, are performed by detecting the recoils in forward direction. In the usual backscattering geometry for channeling RBS the scattered projectiles are detected. For channeling ERDA experiments, one may first use the blocking technique to achieve the desired crystal orientation. Subsequently, the channeling is carried out with the so-aligned sample to get the channeling scan by recording recoils (for a fixed incidence charge) at different angles. The technique has been used to measure the strain^{34,35} at the interface of CoSi₂ and Si crystal. Intensities of recoils of Co and Si (which are separated by each other by the use of telescope detector) are plotted for different angles as shown in Figure 11. The angular scans for Co and Si show two minima in recoil intensities at two different angles. These two angles basically represent the axes of Co and

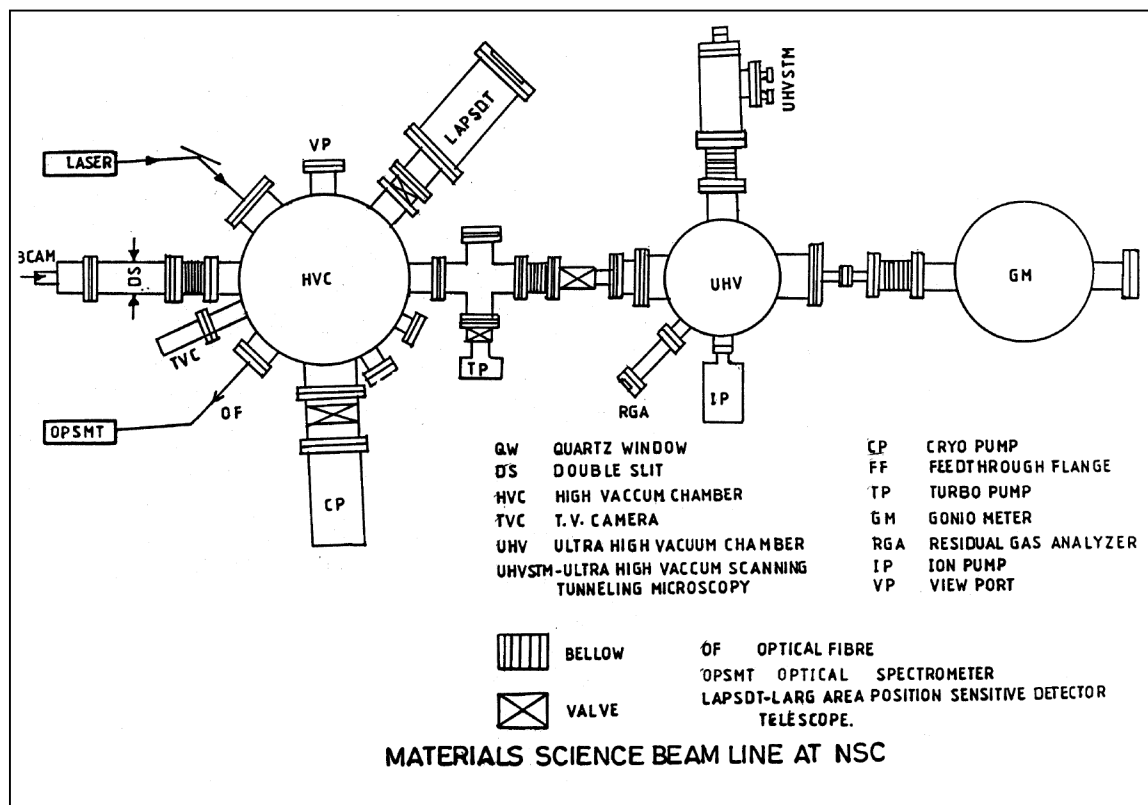


Figure 9. The experimental facilities in materials science beam line at NSC. Telescope detector abbreviated as LAPSMT is shown at 45 degree port of the high vacuum chamber. Other *in situ* and online facilities are also shown. (Reprinted from *Nucl. Instrum. Methods*, Volume number 156, Singh, J. P. *et al.*, Swift heavy ion based materials science research at NSC, p. 587, Copyright (1999), with permission from Elsevier Science.)

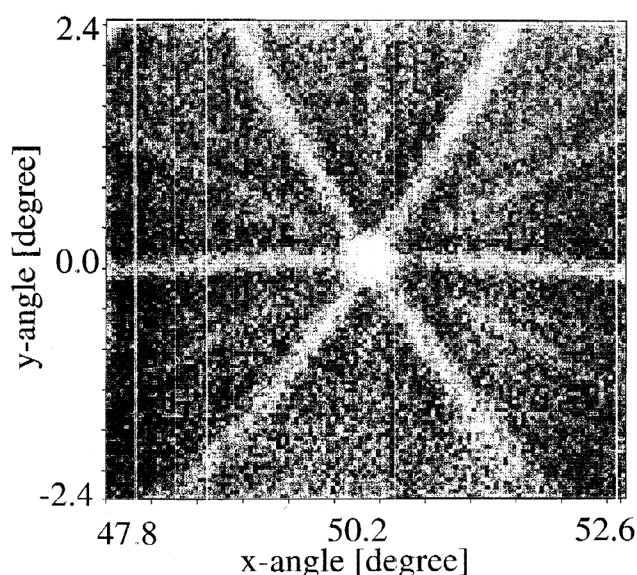


Figure 10. Blocking picture of Si recoils as recorded by two-dimensional position sensitive detector. Si recoils are generated due to the impingement of energetic Au ions. (Reprinted from *Nucl. Instrum. Methods*, Volume number B136–138, Nolte *et al.*, Blocking and Channeling – ERDA with heavy ions, p. 587, Copyright (1998), with permission from Elsevier Science.)

Si in CoSi_2 and that of Si in the Si substrate. The difference in these two angles is a measure of the strain. The main advantage of channeling ERDA compared to channeling RBS is the possibility of distinguishing different crystal components.

5.0 Online monitoring of ion-induced modifications

Heavy ions of high energy (1 MeV/nucleon), often referred as swift heavy ions (SHI) are capable of producing modifications in materials due to their large electronic excitation. On-line monitoring of ion-induced modifications³⁶ is one of the most interesting aspects of the ERDA technique with a large area position sensitive detector. SHI are capable of producing modification at the surface, bulk and the interface of thin films deposited on the substrate. All these three modifications belong to a different branch of study. SHI-induced changes at the surface are investigated to understand some surface science aspects. Electronic sputtering is an area which can be investigated by online monitoring in

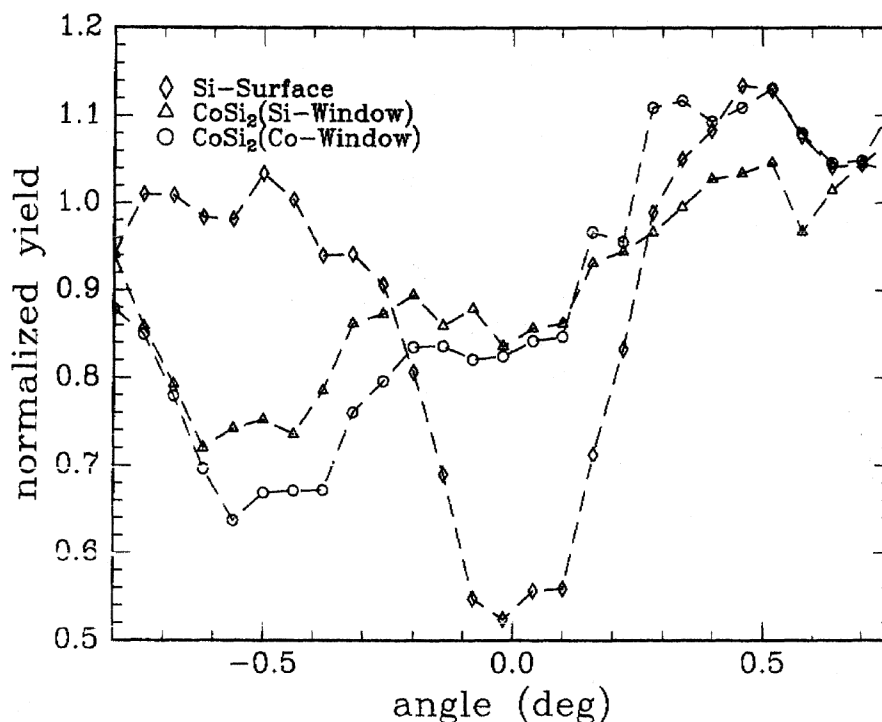


Figure 11. Channeling ERDA spectra of Si and Co of a crystalline CoSi₂ layer and of Si from the Si substrate (Reprinted from *Nucl. Instrum. Methods*, Volume B136–138, Nolte, H. *et al.*, Blocking and Channeling – ERDA with heavy ions, p. 587, Copyright (1998), with permission from Elsevier Science.)

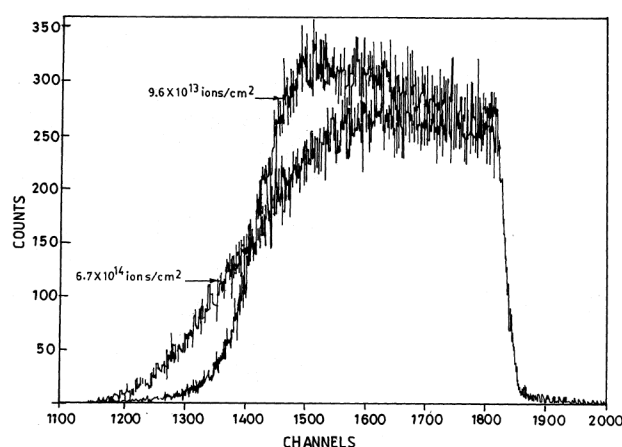


Figure 12. Two Cu recoil spectra recorded for the same incident ion charge at different fluences for the sample of CuO thin film on float glass. Low energy edge of the spectra provides the signature of mixing at the interface. (Reprinted from *Nucl. Instrum. Methods*, Volume B156, Avasthi, D. K. *et al.*, On-line study of ion beam induced mixing at interface by swift heavy ions, p. 143, Copyright (1999), with permission from Elsevier Science.)

specific cases. These two areas (surface modifications by energetic ions and electronic sputtering) belong to surface science studies. Secondly, the modifications at the interface are studied under the topic of ion beam mixing. Thirdly, the modifications in the bulk properties (in terms of electrical, optical, mechanical and structural properties) is of wide interest. The stoichiometric changes in the film especially in the case

of hydrogen and light element constituents are also investigated by online ERDA. Modifications by ion beams at the interface can be produced by ion beam mixing. This has been investigated recently by online ERDA, too. Modifying the sample structure by SHI irradiation and probing it at the same time is thus a unique feature of ERDA channeling.

5.1 Online monitoring of mixing at interface

Ion beam mixing is an important phenomenon related to the modification of an interface by energetic ion beams. The process of mingling the atoms of one layer (or film) with the atoms of other elements in the substrate (or layer/film) at an interface of two layers under the influence of energetic ion beam, is known as ion beam mixing. Ion beam mixing has been of wide interest because of its role in producing novel phases with spatial selectivity, improving the adhesion of films on substrate etc. Conventional ion beam mixing is known to occur with low energy ions in the keV-range where the elastic collision process dominates. It is well known that the amount of mixing at the interface is proportional to the nuclear energy loss resulting from the elastic collisions. The mixing reaches its maximum at energies where the nuclear energy loss is maximum and then it falls down with energy as the nuclear energy loss decreases. It is therefore expected that the mixing will not take place at high energies, i.e. in the energy regime of swift heavy

ions. It has, however, been shown in recent years that swift heavy ions can cause mixing at the interface. First report on swift heavy ion beam induced mixing³⁷ was published in 1993. The study of mixing is also of interest for the understanding of interaction of swift heavy ion with material in general.

It was shown that incident ions produce mixing at the interface and the recoils generated by the incident ions may provide information about the changes at the interface^{38,39}. An example is shown in Figure 12, where Cu recoil spectra indicate the mixing at the interface in an online measurement. A 230 MeV Au ion beam was incident on a CuO film deposited on float glass, which caused mixing of Cu in the float glass. Energetic Au

ions, during its passage through the sample, do the modifications at the interface and produce recoils of Cu (from CuO film) and O (from CuO film and the float glass). These recoils are detected in a telescope detector, which separates the recoils of different masses as discussed in §3.2.3. Figure 12 shows the Cu recoil spectra at different fluences (in the beginning of irradiation and in the end of irradiation). Low energy region of the spectra represents the interface region. The change in this region is indication of the mixing at the interface. In a similar study³⁸, 230 MeV Au ions incident on a thin Fe film deposited on a Si substrate showed the mixing of Fe with Si at the interface, which was monitored online. Online ERD with large area and position sensitive detectors incorporating kinematic correction, provides a unique way of studying such interface processes.

5.2 Online monitoring of electronic sputtering

The impingement of energetic ions on the surface of solids causes the emission of atoms from this surface known as sputtering. The process of sputtering depends on the nuclear energy loss caused by elastic collision cascades. It is therefore expected that the sputtering yield decreases with the increase in energy beyond the nuclear energy loss maximum. However, it has been observed that sputtering increases above a certain threshold of electronic excitation. Such a sputtering process is called electronic sputtering. There have been reports of desorption of light elements such as hydrogen, oxygen etc. from the bulk of certain films under the influence of electronic excitation. Study of the electronic sputtering process is a good means to investigate ion–solid interaction. The desorption of carbon and hydrogen from amorphous carbon films containing hydrogen has been studied^{40–43}. The change in concentrations of H and C with increasing fluence of incident high energy heavy ion beam indicates erosion of the film due to electronic sputtering. This is conveniently recorded by online ERDA. The large sputtering yield has been explained by a transient thermal spike⁴³ generated by the incident ion. It was also observed that the desorption of carbon and hydrogen depends on the structural properties of the film⁴². It is concluded from this study that the erosion process is stronger in the films with low value of I_d/I_g and high hydrogen concentration. I_d and I_g correspond to disordered phase and microcrystalline graphite phase respectively in amorphous carbon network. The ratio of I_d to I_g is determined by the Raman spectroscopic measurements.

Low energy sputtering can also be investigated by ERDA if an ion source is mounted on the chamber used for ERDA experiment. The desorption of surface carbon and oxygen layers on Ti foil due to low energy Xe ions was investigated by Mieskes *et al.*⁴⁴ using *in situ*

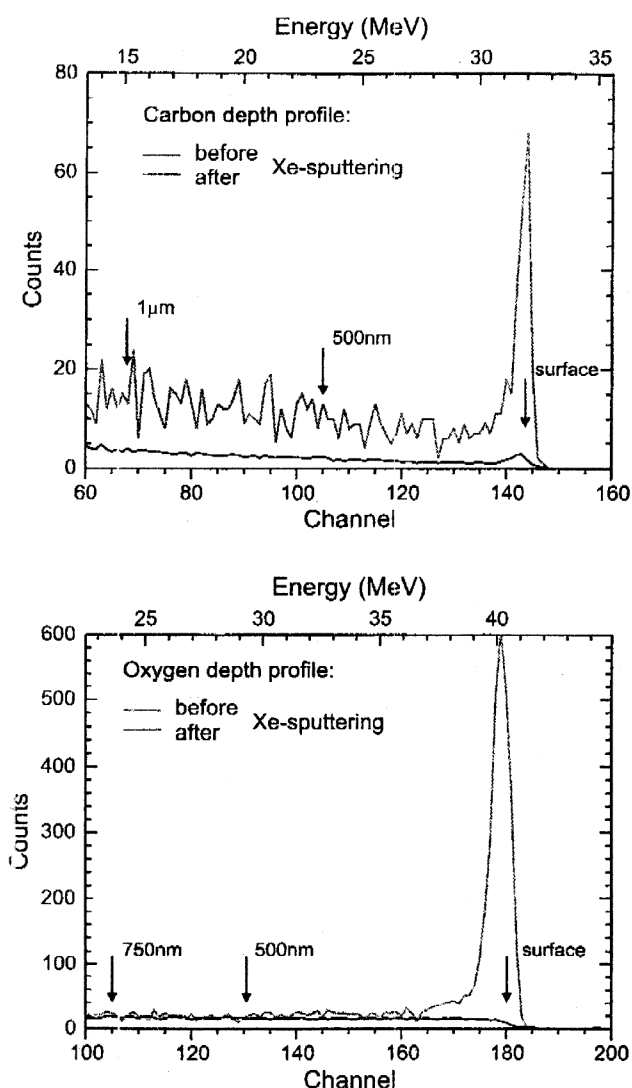


Figure 13. Online monitoring of high energy sputtering by ERDA. Recoil spectra of surface O and C are measured during the irradiation of a Ti sputter target with and without sputter cleaning by 8 keV Xe ions. (Reprinted from *Nucl. Instrum. Methods*, Volume B146, Mieskes, H. D. *et al.*, Measuring sputtering yield of high energy heavy ions on metals, p. 162, copyright (1998), with permission from Elsevier Science.)

ERDA. The recoil spectra of carbon and oxygen before and after 8 keV Xe ion sputtering is shown in Figure 13.

6. Conclusion

Conventional ERDA provides the depth profiling of light elements. The use of detector telescopes in ERDA allowed depth profiling of a wide range of elements up to mass 150 with mass resolution which allows the separation of neighbouring light mass elements. The use of large area position sensitive detectors with kinematic correction has proved to be an excellent means for online monitoring of the SHI induced changes in bulk, surface and at the interface of thin films on a substrate. Apart from its use in materials analysis, it is useful in the study of electronic excitation-induced mixing at the interface, electronic sputtering in some specific cases like insulators, diamond-like carbon films etc. and desorption of hydrogen and other light gaseous elements from the bulk of the samples. The use of two-dimensional position sensitive detector with ERDA technique is helpful in the study of electronic excitation induced damage in single crystals.

1. Chu, W. K., Mayer, J. W. and Nicolet, M. A., *Backscattering Spectrometry*, Academic Press, New York, 1978.
2. Lindhard, J., *Kgl. Danske Vidensk. Selsk. Mat. Fys. Medd.*, 1965, **34**.
3. Gemmel, D. S., *Rev. Mod. Phys.*, 1974, **46**, 129.
4. L'Ecuyer, J., Brassard, C., Cardinal, C. and Terreault, B., *Nucl. Instrum. Methods*, 1978, **B149**, 271.
5. Doyle, B. L. and Pearcey, P. S., *Appl. Phys. Lett.*, 1979, **34**, 812.
6. Jaipal, Kabiraj, D. and Avasthi, D. K., *Nucl. Instrum. Methods*, 1993, **A334**, 196.
7. Kabiraj, D., Mandal, S. and Avasthi, D. K., *Nucl. Instrum. Methods*, 1995, **A362**, 205.
8. Assmann, W. and Maier, H. J., *Nucl. Instrum. Methods*, 1995, **A362**, 143.
9. Avasthi, D. K., *Mater. Sci. Forum*, 1997, **248–249**, 405.
10. Tripathi, A., Choudhury, G. K. and Avasthi, D. K., *Vacuum*, 1997, **48**, 1023.
11. Avasthi, D. K., Acharya, M. G., Tarey, R. D., Malhotra, L. K. and Mehta, G. K., *Vacuum*, 1995, **46**, 265.
12. Whitlow, H. J., Possnert, G. and Petersson, C. S., *Nucl. Instrum. Methods*, 1987, **B27**, 448.
13. Groleau, R., Gujrathi, S. C. and Martin, J. P., *Nucl. Instrum. Methods*, 1983, **218**, 11.
14. Arai, E., Funaki, H., Katayama, M. and Shimizu, K., *Nucl. Instrum. Methods*, 1992, **B68**, 202.
15. Rijken, H. A., Klien, S. S. and Voigt, M. J. A. de, *Nucl. Instrum. Methods*, 1992, **B64**, 395.
16. Thomas, J. P., Fallavier, M., Ramdane, D., Chevarier, N. and Chevarier, A., *Nucl. Instrum. Methods*, 1983, **B218**, 125.
17. Yu, R. and Gustafsson, T., *Surface Sci.*, 1986, **177**, L987.
18. Stoquert, J. P., Guillaume, G., Hage Ali, M., Grob, J. J., Ganter, C. and Siffert, P., *Nucl. Instrum. Methods*, 1989, **B44**, 184.
19. Arnold Bik, W. M. and Harbraken, F. H. P. M., *Rep. Prog. Phys.*, 1993, **56**, 859.
20. Arnold Bik, W. M., Laat, C. T. A. M. de and Habraken, F. H. P. M., *Nucl. Instrum. Methods*, 1992, **B64**, 832.
21. Petrascu, M., Berceanu, I., Brancus, I., Buta, A., Duma, M., Grama, C., Lazar, I., Mihai, I., Peterovici, M., Simon, V., Mihaila, M. and Ghita, A., *Nucl. Instrum. Methods*, 1984, **B4**, 396.
22. Avasthi, D. K., Kabiraj, D., Bhagwat, A., Mehta, G. K., Vankar, V. D. and Ogale, S. B., *Nucl. Instrum. Methods*, 1994, **B93**, 480.
23. Avasthi, D. K., Hui, S. K., Subramaniam, E. T. and Mehta, B. R., *Vacuum*, 1996, **47**, 1061.
24. Boerma, D. O., Labohm, F. and Reinders, J. A., *Nucl. Instrum. Methods*, 1990, **B68**, 291.
25. Dollinger, G., Frey, C. M., Bergmaier, A. and Fastermann, T., *Nucl. Instrum. Methods*, 1998, **B129**, 603.
26. Tripathi, A., Mandal, S., Kataria, D. O., Avasthi, D. K. and Datta, S. K., *Nucl. Instrum. Methods*, 1997, **B129**, 423.
27. Behrisch, R., Grötzschel, R., Hentschel, E. and Assmann, W., *Nucl. Instrum. Methods*, 1992, **B68**, 245.
28. Bromley, D., ed., *Treatise on Heavy Ion Science*, Plenum Press, New York, 1984.
29. Assmann, W., Huber, H., Steinhausen, Ch., Dobler, M., Glückler, H. and Weidinger, A., *Nucl. Instrum. Methods*, 1994, **B89**, 480.
30. Davies, J. A., Foster, J. S. and Walka, S. S., *Nucl. Instrum. Methods*, 1998, **B136–138**, 594.
31. Timmers, H., Ophel, T. R. and Elliman, R. G., *Nucl. Instrum. Methods*, 1999, **B156**, 236.
32. Huber, H., Assmann, W., Karamian, S. A., Mieskes, H. D., Nolte, H., Gazis, E., Kokkoris, M., Kossionides, S., Vlastou, R., Grotzschel, R., Muklich, A. M. and Prusseit, M., *Nucl. Instrum. Methods*, 1998, **B146**, 309.
33. Huber, H., Assmann, W., Karamian, S. A., Mücklich, A., Prusseit, W., Gaiz, E., Grötzschel, R., Kokkoris, M., Kossionidis, E., Mieskes, H. D. and Vlastou, R., *Nucl. Instrum. Methods*, 1997, **B122**, 542.
34. Assmann, W., Annual Report Tandem Accelerator Laboratory, 1997.
35. Nolte, H., Assmann, W., Huber, H., Karamian, S. A. and Mieskes, H. D., *Nucl. Instrum. Methods*, 1998, **B136–138**, 587.
36. Avasthi, D. K., Assmann, W., Huber, H., Mieskes, H. D. and Nolte, H., *Nucl. Instrum. Methods*, 1998, **B142**, 117.
37. Dufour, C., Bauer, Ph., Marchal, G., Grihle, J., Jaouen, C., Paccaud, J. P. and Jousset, J. C., *Euro. Phys. Lett.*, 1993, **1**, 671.
38. Avasthi, D. K., Assmann, W., Mieskes, H. D., Nolte, H., Tripathi, A. and Ghosh, S., *Nucl. Instrum. Methods*, 1999, **B156**, 143.
39. Avasthi, D. K., Assmann, W., Nolte, H., Mieskes, H. D., Ghosh, S. and Misra, N. C., *Nucl. Instrum. Methods*, 2000, **B166–167**, 345.
40. Dollinger, G., Boulouedine, M., Bergmaier, A., Faestermann, T. and Frey, C. M., *Nucl. Instrum. Methods*, 1996, **B118**, 291.
41. Behrisch, R., Prozesky, V. M., Huber, H. and Assmann, W., *Nucl. Instrum. Methods*, 1996, **B118**, 262.
42. Ghosh, S., Avasthi, D. K., Ingale, A., Tripathi, A., Som, T., Kabiraj, D., Zhang, S., Proceedings of DAE symposium on Solid State Physics, 1999.
43. Pawlack, F., Dufour, Ch., Laurent, A., Paumier, E., Perriere, J., Stoquert, J. P. and Toulemonde, M., *Nucl. Instrum. Methods*, 1999, **B151**, 140.
44. Mieskes, H. D., Assmann, W., Brodale, M., Dobler, M., Glucker, H., Hartung, P. and Stenzel, P., *Nucl. Instrum. Methods*, 1998, **B146**, 162.

ACKNOWLEDGEMENTS. We thank BMBF Bonn and Department of Science and Technology for the financial support to the Indo-German project on 'High energy heavy ion beam mixing and sputtering'. D.K.A. thanks the Department of Science and Technology for financial support to set up the experimental facilities for research in the field of materials science.